Sustainable Water-Energy Management in Microgrid-Driven BWRO Desalination Prototype Considering Technological Constraints

Mehdi Turki, Jamel Belhadj, Xavier Roboam

Smart Grids and Sustainable Energy _####################_
https://doi.org/10.1007/s40866-023-00189-8

ORIGINAL PAPER

Sustainable Water-Energy Management in Microgrid-Driven BWRO Desalination Prototype Considering Technological Constraints

Mehdi Turki[1,2] · Jamel Belhadj[1,3] · Xavier Roboam[4]

Received: 15 July 2023 / Accepted: 18 December 2023

Abstract

This article delves into the exploration of a Brackish Water Reverse Osmosis (BWRO) desalination system, powered by a renewable microgrid that operates without the need for electro-chemical energy storage. The study takes a comprehensive approach, focusing on the Water-Energy nexus, with an emphasis on identifying operational constraints through an experimental BWRO prototype. The desalination system applies a "power-sharing" strategy alongside Power Field Oriented Control (PFOC) to ensure safe operation within pressurized systems. The integration of technological limitations establishes a "Safe Operation Window (SOW)" while accommodating fluctuations in renewable energy production. The ultimate objective is to optimize freshwater production capacity, considering the constraints of both microgrid electrical power and the BWRO unit. Real-time management of Water-Energy is facilitated by an Energy Management System (EMS), which maximizes water production and minimizes energy consumption under varying climatic conditions. In summary, this research offers valuable insights into sustainable water production through the utilization of renewable microgrids and innovative control strategies. The "power-sharing" approach, coupled with precise control of motor pump modes, significantly contributes to enhanced system efficiency. This study underscores the importance of addressing the Water-Energy nexus in the context of desalination for sustainable water supply.

Keywords Water-Energy nexus · BWRO desalination prototype · Standalone microgrid · Safe Operating Window · Energy Management System

✉ Mehdi Turki
Turki.mehdi@gmail.com

Jamel Belhadj
Jamel.Belhadj@esstt.rnu.tn

Xavier Roboam
Xavier.Roboam@laplace.univ-tlse.fr

[1] LR 11 ES 15, Ecole Nationale d'Ingénieurs de Tunis, Laboratoire Des Systèmes Electriques, Université de Tunis El Manar, BP 37 – 1002, Le Belvédère, Tunis, Tunisia

[2] Ecole Supérieure Des Ingénieurs de Medjez El Bab, Université de Jendouba, 9070 Medjez El Bab, Tunisia

[3] Ecole Nationale Supérieure d'Ingénieurs de Tunis, Université de Tunis, BP 56 – 1008, Montfleury, Tunisia

[4] LAPLACE (Laboratoire Plasma Et Conversion d'Énergie), UMR CNRS-INP-UPS, ENSEEIHT, Université de Toulouse, 2 Rue Camichel 31071, Toulouse, France

Nomenclature

Acronyms

BWRO	Brackish Water Reverse Osmosis
CV	Control Valve
DC	Direct Current
EMS	Energy Management System
NF	Nanofiltration
HP	High Pressure
LP	Low Pressure
IM	Induction motor
MPPT	Maximum Power Point Tracking
PFOC	Power Field Oriented Control
PV	Photovoltaic
PWM	Pulse Width Modulation
RES	Renewable Energy Source
RO	Reverse Osmosis
SOW	Safe Operation Window
SWRO	Seawater Reverse Osmosis
VFD	Variable Frequency Drive
VSI	Voltage Source Inverter
WP	Welling pump

Symbols/variables/parameters

A_o	Reference water permeability
A_t	Water permeability at temperature t ($kg\ s^{-1}\ Pa^{-1}\ m^{-2}$)
B_o	Reference salt permeability
B_t	Salt permeability at temperature t ($kg\ s^{-1}\ Pa^{-1}\ m^{-2}$)
I_m	Rotor current (A)
P_p	Water discharge pressure (Pa)
Q_p	Freshwater flow membrane element ($m.s^{-1}$)
Q_r	Reject flow across the membrane element ($m.s^{-1}$)
R_m	Rotor resistance (Ω)
T_m	Electromagnetic torque (N.m)
V_m	Rotor voltage (V)
f_{mp}	Motor and pump mechanical frictions
$\mathscr{P}_{DC}$	Generated power transferred via a DC bus (W)
μ_0	Reference water viscosity
μ_t	Water viscosity at temperature t (mPa·s)
ϕ_m	Excitation magnetic flux (Wb)
ΔC_2	Water concentration difference across the membrane, ($kg\ m^{-3}$)
ΔP	Pressure drop across the membrane element (Pa)
Δπ	Osmotic pressure membrane element drop (Pa)
C_f	Feed water concentration ($kg\ m^{-3}$)
C_p	Freshwater concentration ($kg\ m^{-3}$)
C_r	Reject water concentration ($kg\ m^{-3}$)
d	Water density ($kg\ m^{-3}$)
S	Membrane surface (m^2)
t	Water temperature (K)
t_0	Reference water temperature
Q	Water flow rate ($m.s^{-1}$)
Ω	Rotational speed, $rad.s^{-1}$
α	Power sharing factor

Introduction

AQ2 The concept of "safe drinking water" refers to water that meets the standards for consumption and food preparation. Although large, centralized treatment systems effectively supply urban areas, delivering clean drinking water to remote and rural locations poses greater challenges and higher costs. Remote communities often face the scarcity or poor quality of drinking water. In 2020, approximately 25% of the world's population did not have access to safely managed drinking water in their residences, and almost 50% lacked adequate sanitation facilities. The COVID-19 pandemic has underscored the critical importance of ensuring access to adequate hand hygiene. At the outset of the pandemic, three out of every ten people worldwide were unable to wash their hands with soap and water in their own homes [1].

Desalination processes primarily involve membrane-based procedures utilizing pressure differences or thermal processes based on phase change. Thermal distillation methods, such as multi-stage, multi-effect, and vapour compression flash, are employed to extract freshwater. Reverse osmosis (RO) desalination, utilizing filtration membranes, is the most widely used technology in the industry. RO operates by selectively permeating a saline solution through a semi-permeable membrane under pressure, resulting in the separation of liquid phases [2–5].

Recent research on water desalination indicates that renewable energy accounts for only 1% of total desalinated water production. To address water scarcity in remote areas, an effective approach involves integrating desalination technology with renewable energy sources (e.g., wind and solar power). Desalination processes powered by renewable electricity systems can reduce reliance on fossil fuels and minimize greenhouse gas emissions. The global market potential for desalination systems utilizing renewable energy is significant due to the increasing demand for freshwater [6].

The Water-Energy nexus represents a promising approach to tackle the challenges associated with the scarcity of these essential resources. It provides a sustainable and environmentally beneficial solution, particularly in areas with limited hydraulic and electrical infrastructure but abundant renewable energy sources. RO desalination technologies, driven by photovoltaic and/or wind power, play a critical role in this combination. A cost study conducted on 81 projects in the Middle East revealed a 20% reduction in power production costs and a 4% reduction in water desalination prices [7, 8].

Many research studies have delved into various facets of freshwater production using renewable energy sources. These investigations have covered topics such as system design, control and management strategies for water-energy, as well as optimization methods [9, 10]. However, in most studies on RO desalination powered by renewable sources, concerns regarding the control and management of critical system components, particularly membrane efficiency, as well as technical and technological process performance, are frequently highlighted. These crucial aspects necessitate special attention to optimize the desalination system's operation and ensure the effective and reliable production of freshwater.

In this study, a prototype of Brackish Water desalination using RO technology powered by a standalone renewable microgrid (PV-Wind) without the need for electro-chemical storage is investigated. To meet the freshwater needs for various applications, hydraulic storage in water reservoirs will be employed as a superior alternative to battery storage. This substitution holds significant importance due to its several advantages, such as increased storage capacity,

Journal : Large 40866 | Article No : 189 | Pages : 18 | MS Code : 189 | Dispatch : 28-12-2023

reduced environmental impact, and enhanced reliability in meeting fluctuating water demand. The control and management of Water-Energy necessitates the development of an experimental test approach and quasi-static models of the overall system. Specifically, this paper focuses on identifying the operating window of the RO membrane, pressurization systems, and water storage reservoir for different salinities and temperatures of Brackish water. This operating window will determine the electrical limits when utilizing a fluctuating and intermittent electrical source, which will be shared among motor-pumps. A Water-Energy management approach, developed in this work, will optimize, and maximize freshwater production based on instantaneous electrical power provided by the hybrid renewable source.

Literature review: Technological Constraints of RO Desalination Processes

Due to the high sensitivity of polyamide RO membranes, membrane module manufacturers recommend operating at a constant water flow and pressure to minimize membrane damage and extend the lifespan of the process. However, when a RES is used, the operation of the RO system is subject to variable and fluctuating hydro-mechanical quantities due to the unpredictability and intermittency of solar and/or wind energy. As a result, the RO process and associated pressurizing subsystems can be operated within a range of operating conditions, rather than a fixed operating point. This concept, known as the operating window (SOW), was first introduced by Feron [11], which defined the extreme boundaries within which a membrane can be safely operated.

Several research studies have investigated the feasibility of implementing the SOW concept in RO desalination systems coupled with RES, although the analysis of performance data has been limited. For instance, Miranda et al. [11] presented an analysis of a small-scale seawater reverse osmosis (SWRO) desalination unit powered by a 2.2 kW autonomous wind generator without batteries, aiming to reduce investment and operating costs. In this study, an operational window was defined to determine the allowable fluctuations in operational parameters that the membrane can safely withstand. The average freshwater production capacity was approximately 8.5 m3/day, and the specific energy consumption of the system was approximately 3.4 kWh/m^3, which appears to be relatively low compared to existing literature. Based on the power output of the wind turbine, a control strategy was devised to operate the RO unit within the defined operating window. Miranda et al. proposed two additional options for powering a stand-alone RO unit in this study, both of which did not involve storage or backup technologies such as diesel generators, but rather relied on RO unit ON/OFF switching.

Gilau et al. [12] examined the cost-effectiveness of a stand-alone seawater reverse osmosis system powered by photovoltaic energy or wind turbines with batteries, targeting underdeveloped countries. The HOMER software was used to simulate hourly electricity output from the RES micro-grid. The drinking water production of 35 m^3/day was estimated using the ROSA membrane manufacturer's software. To account for intermittent power supply, an operational window was introduced, enabling the RO system to operate under fluctuating power conditions. The simulation results indicated that wind systems had the lowest Net Present Cost (NPC) for a given location. Additionally, in the case of PV-powered RO systems, the usage of batteries had a significant impact on water production. The contributions of booster pumps and energy recovery devices to increased water production and reduced energy consumption per cubic meter of water generated were found to be substantial. These findings demonstrated the possibility of freshwater production at a specific energy consumption of 2.33 kWh/m^3 using currently available technology.

Pohl et al. [13] presented a theoretical analysis of various operational solutions for variable SWRO module operations. Based on simulation results using the ROSA software, they concluded that operating with a constant recovery rate represents the best compromise compared to operating with constant feed water pressure, constant feed water flow, or constant reject water flow. The recommended variable operating methods can be implemented using the approach described in this study.

Park et al. [14–16] investigated the potential of supercapacitors to expand the operating window of a wind-powered RO membrane system. By conducting experiments using a BWRO desalination system, they discovered that utilizing supercapacitors enhanced power reliability, leading to higher average water flow and improved freshwater quality. By buffering wind fluctuations with an oscillation time of 1 min, the average flux was increased by 85%, and the quality of the permeate produced over a 10-min period improved by 40% compared to a direct-drive system without energy storage. The supercapacitors provided steady power to the membrane system, resulting in enhanced power delivery and improved system performance. The capacity of the supercapacitor bank determined the duration of power supply during intermittent periods.

Shen et al. [17] and Richards et al. [18] conducted experimental studies to determine the operating window of a RES-powered BWRO desalination system. The focus of their research was on a photovoltaic membrane system with a direct connection, subject to fluctuating solar conditions. Two designs of nanofiltration (NF)/RO membranes with the same membrane area were extensively studied.

A battery less PV-powered membrane system with two module sizes was operated under energy fluctuations. The operating parameters (pressure, feed rate) and performance indicators (flow, permeate salinity) of the two modules were compared. The resulting SOW was defined as a pentagon constrained by a minimum set-point of back-pressure valve, maximum recovery rate, maximum pump power, maximum set-point of back-pressure valve, and minimum recovery rate. The study also demonstrated that the SOW depends on the feed water salinity and membrane type. Various operating strategies were investigated to maximize performance under variable electrical power, and the constant recovery rate strategy was found to produce the highest flux with the lowest specific energy consumption, while maintaining good retention.

Ruiz-Garca et al. [19–21] studied the 14-year performance of a RO desalination plant operating under intermittent conditions. They proposed a simple on–off control method for a variable power-fed BWRO system with one or two stages, considering different configurations with six spirally wrapped membrane elements per pressure vessel. By simulating variations in feed water quality from a real groundwater well and analysing the reaction of different configurations, they aimed to select the most suitable one based on the available electrical power for the BWRO system.

Furthermore, the literature research revealed that in most cases, the SOW operating strategy limits the maximum capacity of a RO desalination unit powered by a RES (with or without a battery). If the required power supply cannot be achieved, the installation will be turned OFF.

The corrected section of the paper sheds light on the operational strategies of reverse osmosis (RO) desalination systems powered by renewable energy sources. It highlights the importance of analysing the system's operating window (SOW) to optimize performance and preserve the integrity of sensitive RO membranes. The examined research studies explore various approaches, such as harnessing wind or solar energy, integrating supercapacitors, and utilizing energy recovery, to adapt the system operation to power fluctuations. These approaches have demonstrated the potential to efficiently produce freshwater using renewable energy sources. The information presented in this section is valuable to researchers, engineers, and decision-makers, providing practical insights for guiding the design and operation of sustainable and energy-efficient desalination systems. It emphasizes the significance of understanding the operating window to prevent membrane damage and extend the lifespan of the desalination process. Overall, this enhanced section of the scientific paper enhances our understanding of operational strategies for renewable energy-powered RO desalination systems, providing practical knowledge to advance sustainable freshwater production technologies.

Experimental Prototype Overview: Design and Setup of the RO Desalination System

The experimental prototype of a standalone brackish water reverse osmosis (BWRO) desalination system (Fig. 2) was developed as a pilot project with a maximum production capacity of approximately 7.2 m^3/d. This system was designed to be powered by a standalone renewable microgrid and aimed at addressing freshwater production needs in remote communities. The experimental setup was constructed at the L.S.E laboratory in Tunis, Tunisia (Fig. 1). AQ3

The standalone BWRO system consists of three main parts:

Part 1: The RES system incorporates a 2 kW solar generator and a 2 kW wind turbine, connected through a DC bus. The hybrid PV/wind system utilizes the Maximum Power Point Tracking (MPPT) technique to maximize power extraction. The generated power ($\mathcal{P}_{DC}$) is variable based on wind speed and solar irradiation conditions. In the absence of battery storage, the PFOC approach is employed in each motor-pump to maintain a steady bus voltage (V_{DC}).

Part 2: The WP subsystem consists of a single-stage centrifugal motor-pump (Motor-pump LP) responsible for pumping brackish water into the feed storage tank. The motor-pump LP is controlled by a three-phase induction motor with a PFOC control system.

Part 3: The pressurizing and filtration system comprises a multi-stage centrifugal motor-pump (Motor-pump HP), a three-phase induction motor with PFOC control, a reverse osmosis (RO) water treatment module, and a hydraulic Control Valve (CV). The motor-pump HP is utilized to boost the pressure of the feed water. Freshwater permeates through the RO membrane and is collected through the permeate tube when the applied pressure exceeds the osmotic pressure, while reject water is drained away.

The hydraulic BWRO desalination system architecture (Fig. 2) depicts two separate hydraulic subsystems, which are decoupled by an elevated water storage tank (T1). Brackish water pumped from the well can be stored in tank T1 when renewable energy is available, either for later use or immediate freshwater production through the RO desalination process. In the absence of renewable energy, the water is stored in tank T2.

To ensure efficient control and management of the electrical power, the "dSPACE DS1104" fast prototyping controller board is employed. Various sensors are deployed to measure hydraulic and electrical variables, which are acquired through the board's analogue inputs [22–24].

Journal : Large 40866 | Article No : 189 | Pages : 18 | MS Code : 189 | Dispatch : 28-12-2023

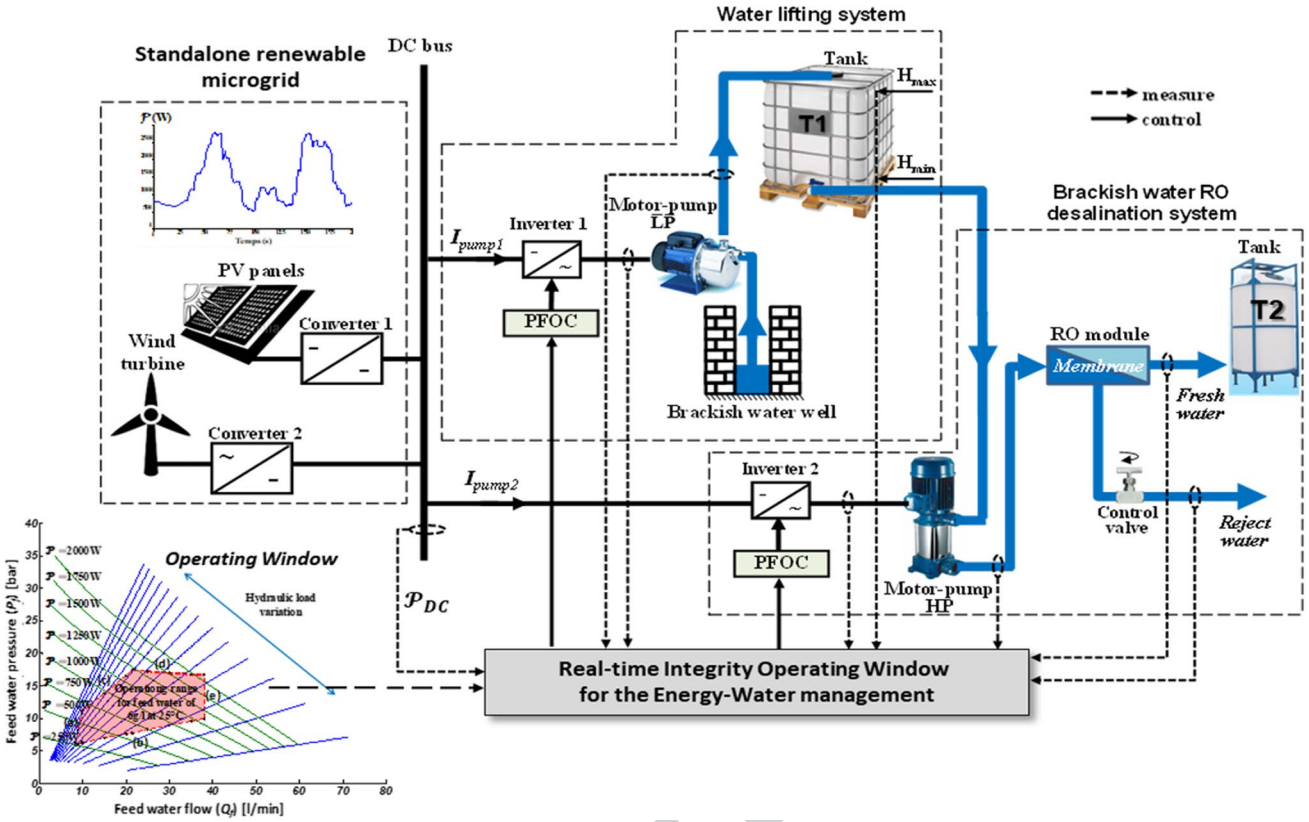

AQ4 AQ5 **Fig. 1** BWRO desalination system configuration

The experimental prototype and its setup allow for thorough testing and investigation of freshwater production using the standalone renewable microgrid system. This research contributes to understanding the feasibility and performance of such systems for remote communities in need of sustainable and reliable freshwater sources.

The analogue output signal from the "dSPACE" board is routed through the VFD (Variable Frequency Drive) "Santerno—Sinus N" to control Pump-w, which is a "LOWARA CEA70/3" pump (Table 1). The VFD controls the power of Pump-w using an electric power regulation loop, leveraging the VFD's analog inputs and PI controller block. For Pump-HP, which is an "EBARA EVM2 22F/2.2" pump (refer to Table 1), PWM (Pulse Width Modulation) signals from the "SEMIKRON VSI" inverter are used to stabilize the DC bus voltage during battery removal.

To remove suspended particles from the supply water, a pre-treatment filter is utilized. The experimental pilot includes one RO membrane, specifically the "TORAY TM710" membrane (Table 2). The hydraulic Control Valve (CV) is set to achieve a maximum recovery rate ($Y = 20\%$). With this configuration, the pilot unit can produce up to 300 L/h of freshwater with a salinity below 100 mg/L using a single filtering membrane.

Under nominal operating conditions with a typical electrical power supply, the total power absorbed by the system is 3270 W. To facilitate the behavioural investigation of the experimental pilot and analyse practical data obtained, the hybrid renewable source can be replaced by a programmable DC power supply. This emulated source allows for the generation of variable power, reaching a maximum value of 4 kW (Table 3). This capability simplifies the analysis of the experimental pilot's behaviour and the examination of practical data.

The experimental pilot unit being investigated falls under the category of complex energy systems. The system's complexity arises from the interplay of multiple components and their functions. This heterogeneity gives rise to the coexistence of various physical phenomena and necessitates considering system constraints from multiple domains to ensure the safe control of the entire system.

Quasi-Static Modelling and Validation of the Hydro-Mechanical Process

The data collected from the experimental prototype will serve as the basis for developing energy models that are essential for determining the safe operating window. These

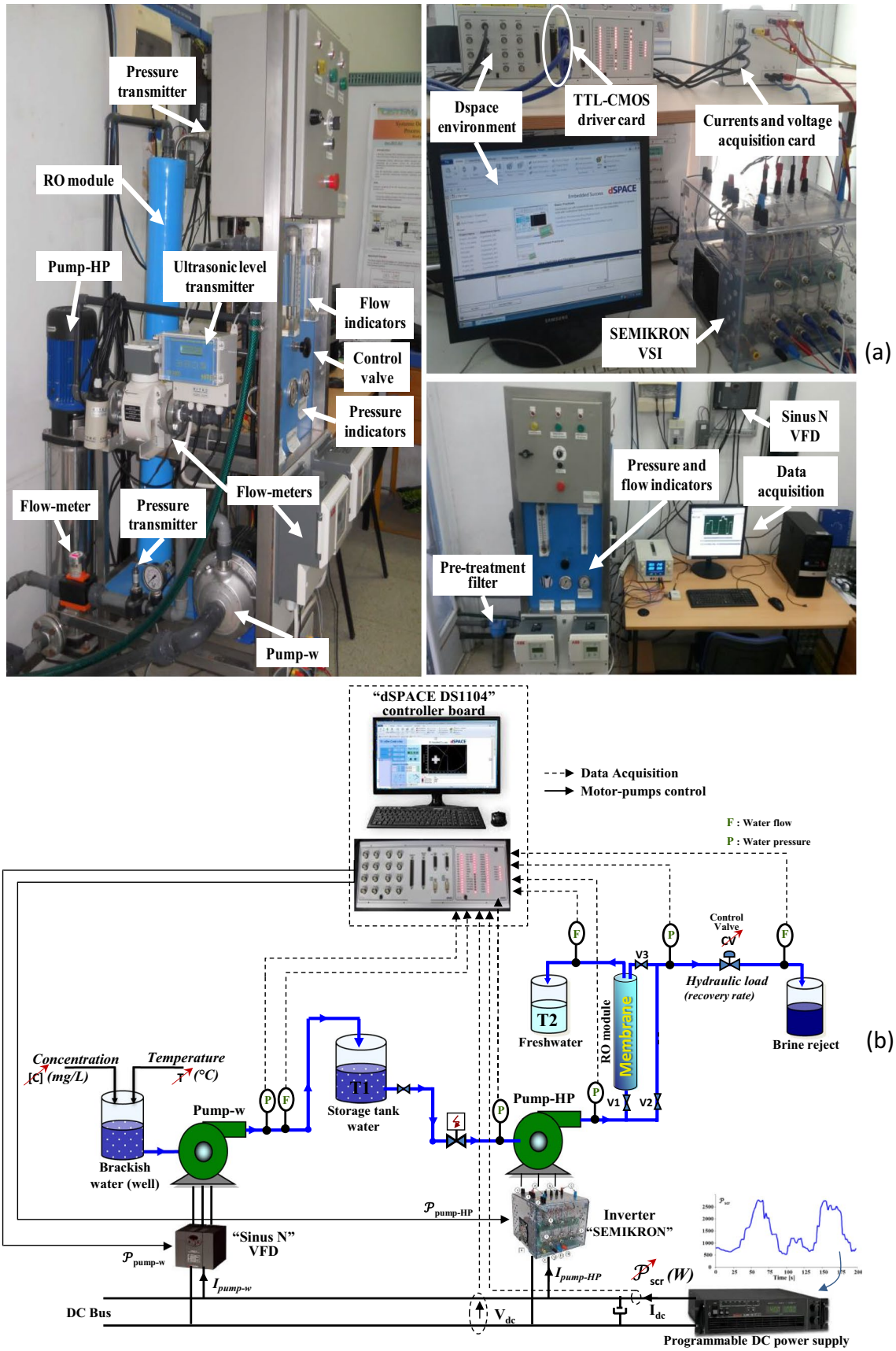

Fig. 2 Experimental BWRO desalination prototype (**a**) and schematic synoptic (**b**)

Table 1 Rated values of the motor-pumps

Motor pump-w	Motor pump-HP
LOWARA CEA70/3	EBARA EVM2 22F/2.2
370 W	2200 W
3 Phases, 50 Hz	
230 V—2.51 A	230V—8.71 A
2820 rpm	2860 rpm
30–80 l/min	20—60 l/min
1.3–2 bar	8.17–18.6 bar

Table 2 RO membrane parameters

Reference	TORAY TM710
Diameter—Area	4"—8 m^2
Minimum salt rejection	99.7%
Freshwater nominal flow	4.5 L/min
Maximum operating pressure	21 bar
Maximum recovery rate	20%
Maximum water temperature	45 °C
Brackish water pH range	2–11

Table 3 Programmable DC Power Supply Technical Information

Reference	Sorensen DLM 600–6.6A 4 kW
Output DC power range	0—3960W
Output DC voltage range	0—600 V
Output DC current range	0—6.6 A

models will enable effective global system control and Water-Energy management.

The quasi-static model, known as a "power flow model," is derived from the dynamic energy behaviour of the desalination chain, considering the electromechanical conversion systems involved. This model considers various physical domains, including motor-pumps, RO processes, and hydraulic stresses (Fig. 3) [25, 26].

To establish the parameters for each centrifugal motor-pump, practical tests were conducted, yielding diverse empirical data. The RO membrane model was developed using equations and principles that accurately represent the flow of materials through the membrane.

By incorporating these models into the analysis, the safe operating window of the RO desalination system can be precisely determined. This information will contribute to efficient Water-Energy management and enable the implementation of reliable control strategies for the entire system. It is worth noting that further details regarding the equations, principles, and experimental procedures used to develop these models would provide a more comprehensive understanding of the research approach.

Centrifugal Motor-Pumps Modelling

The motor-pump modelling principle is to determine the water "flow" and "pressure" for a given electrical power. The static model of a centrifugal pump is represented by the following equations [27, 28]

$$P_p = (a \cdot \Omega + b \cdot Q) \cdot \Omega + c \cdot Q^2 \quad (1)$$

$$T_m = (a \cdot \Omega + b \cdot Q) \cdot Q + (f_{mp}) \cdot \Omega \quad (2)$$

To establish the relationship between electrical power, hydraulic power, and the load characteristic $P_p(Q)$, one must refer to the motor-pump equations. The equation below may deduce the following from Eq. 1:

$$a \cdot \Omega^2 + b \cdot Q \cdot \Omega + c \cdot Q^2 - P_p(Q) = 0 \quad (3)$$

Solving this equation is based on determining the rotation speed as a function of water flow:

$$\Omega(Q) = \frac{-b \cdot Q + \sqrt{(b \cdot Q)^2 - 4 \cdot a \cdot \left[c \cdot Q^2 - P_p(Q)\right]}}{2 \cdot a} \quad (4)$$

From Eq. 2 and Eq. 4, the motor torque can be determined based on water flow rate only: $T_m(Q)$.

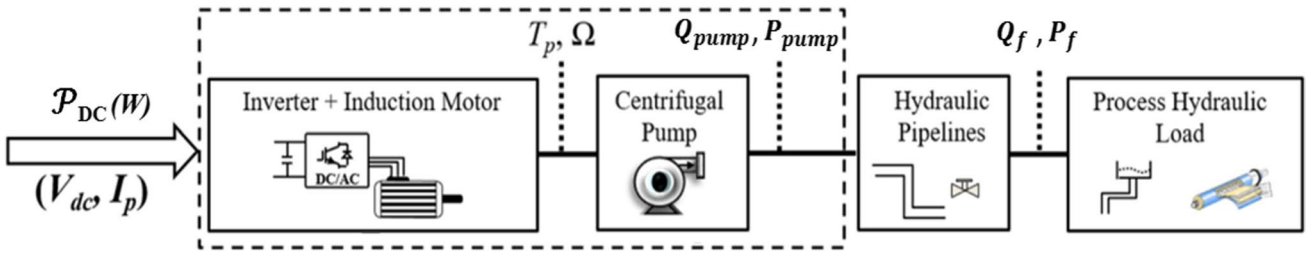

Fig. 3 Quasi-static power flow model of a single motor-pump hydro mechanical process

To validate the motor-pump models, experimental tests were conducted using a variable frequency drive (VFD) to control the motor-pump speeds. A comparison between the experimental data and the model results is shown in Fig. 4, confirming the accuracy of the models.

The motor-pump control is based on a Field-Oriented Control (FOC) method, which decouples the magnetic flux and torque control, making the induction motor control like a DC motor. This allows an equivalent analytical model of the DC motor to be used in conjunction with the centrifugal pump model.

The static model of a DC motor is represented by Eqs. (5) and (6), which describe the relationship between voltage, current, torque, and angular speed. The power of the motor-electrical pump is expressed as a function of angular speed and electromagnetic torque in Eq. (7):

$$V_m = R_m \cdot I_m + \phi_m \cdot \Omega \tag{5}$$

$$T_m = \phi_m \nu I_m \tag{6}$$

$$\mathcal{P}_M = V_m \cdot I_m = \left(R_m \cdot \frac{T_m}{\phi_m} + \phi_m \cdot \Omega \right) \cdot \frac{T_m}{\phi_m} \tag{7}$$

If the torque and speed are replaced in Eq. 3 by their expression as a function of the flow rate, an equation of the electric power was finally obtained, and which depends on only one variable which is the water flow.

By replacing the torque and speed with their expressions as functions of the flow rate, Eq. (8) provides a direct relationship between the electrical power given and water flow rate of the motor-pump for a fixed hydraulic head. Figure 5 depicts the water flow evolution for the motor-pump-w and the motor-pump-HP in relation to the electrical power, based on a combination of analytical modelling and experimental data obtained from the desalination prototype.

$$\mathcal{P}_M\big(\Omega(Q), T_m(Q)\big) = \mathcal{P}_M(Q) \tag{8}$$

The quasi-static models of the motor-pumps demonstrate their coherence with water and energy aspects, highlighting the

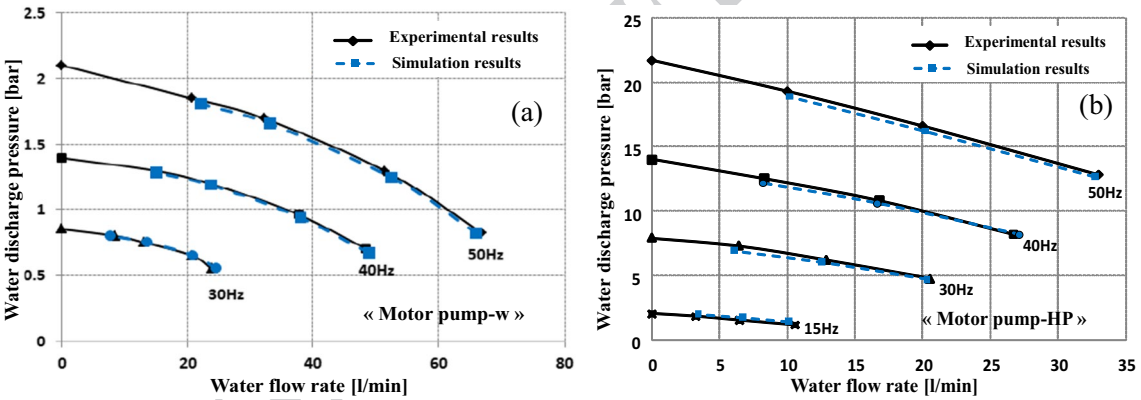

Fig. 4 Comparative Analysis of Centrifugal Motor-Pump Models and Experimental Findings

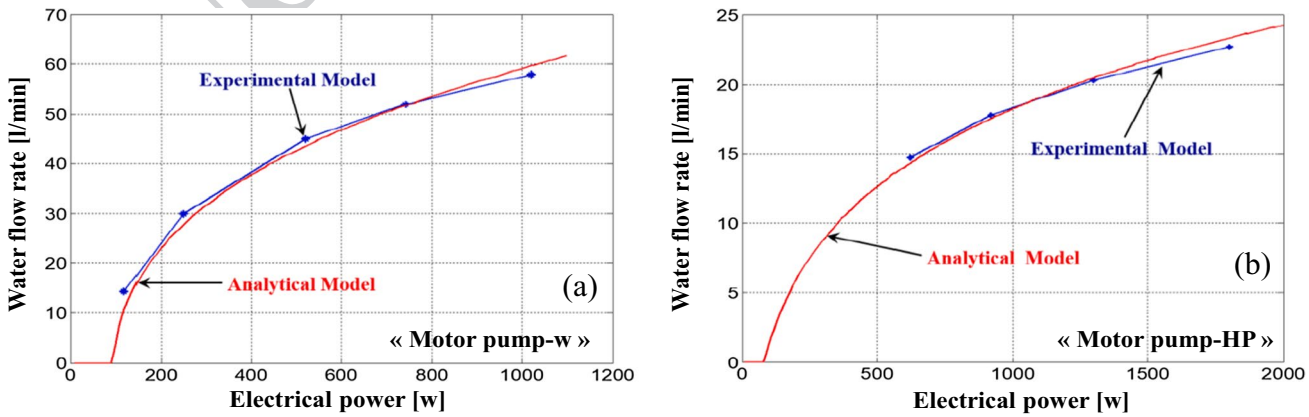

Fig. 5 Water flow evolution for the motor-pumps in relation to electrical power

Journal : Large 40866 | Article No : 189 | Pages : 18 | MS Code : 189 | Dispatch : 28-12-2023

importance of these models in defining the SOW and developing effective Water-Energy management techniques.

RO Membrane Modelling

The RO membrane model was developed based on equations and laws modelling the material transfer through the membrane [27, 29–35].

$$Q_p = \frac{A_t \cdot S}{d} \cdot (\Delta P - \Delta \pi) \tag{9}$$

$$Q_r = \frac{B_t \cdot S}{d} \cdot \Delta C_2 \tag{10}$$

The following equations result from the mass and flow balance:

$$C_r = \frac{C_f \cdot Q_f - C_p \cdot Q_p}{Q_r} \tag{11}$$

$$Q_r = Q_f - Q_p = (1 - Y) \cdot Q_f \tag{12}$$

The water recovery rate:

$$Y = \frac{Q_p}{Q_f} \cdot 100 \tag{13}$$

Temperature influence on membrane properties is represented below:

$$A_t = A_0 \cdot \frac{\mu_0}{\mu_t} \tag{14}$$

$$B_t = B_0 \cdot \frac{\mu_0}{\mu_t} \frac{t_0}{t} \tag{15}$$

Meticulously designed to facilitate comprehensive testing of the subsystem, this experimental prototype boasts versatility, enabling seamless repetition of tests and offering a robust physical model. Importantly, the model integrates established chemical and thermal parameters, providing a holistic perspective on the RO membrane's behaviour under various conditions. The prototype allows for the development of multiple tests for the reverse osmosis (RO) desalination subsystem by varying raw water salinity levels (2, 4, and 6 g/L) and adjusting the control CV (hydraulic load). This approach represents hydraulic quantity evolution and facilitates test repetition using a physical model with previously developed chemical and thermal parameters.

The figure below illustrates the influence of feed pressure (P_f) on both freshwater flow (Q_p) and reject water flow (Q_r) for three different salinity levels, combining experimental data and numerical simulations conducted on MATLAB for a comprehensive representation of the subsystem's performance across various operating conditions.

The insights gleaned from Fig. 6 offer a comprehensive perspective on the evolving behaviour of the desalination unit, specifically focusing on the dynamics of freshwater and reject water flow rates (Q_p, Q_r) in response to varying supply pressure (P_f). What becomes evident is the discernible augmentation of both Q_p and Q_r with increasing P_f. Notably, the influence of pressure on Q_p surpasses that on Q_r, providing a nuanced understanding of the interplay between supply pressure and these crucial flow parameters. This observation substantiates a direct proportionality between the recovery rate (Y) and the supply pressure (P_f), a pivotal aspect in the validation of the unit's performance.

Furthermore, Fig. 7 provides a detailed analysis of the desalination process, elucidating the nuances of how variations in feed pressure (P_f) impact the quality of produced freshwater (C_p), specifically in terms of salt concentration. The results highlight the relationship between feed

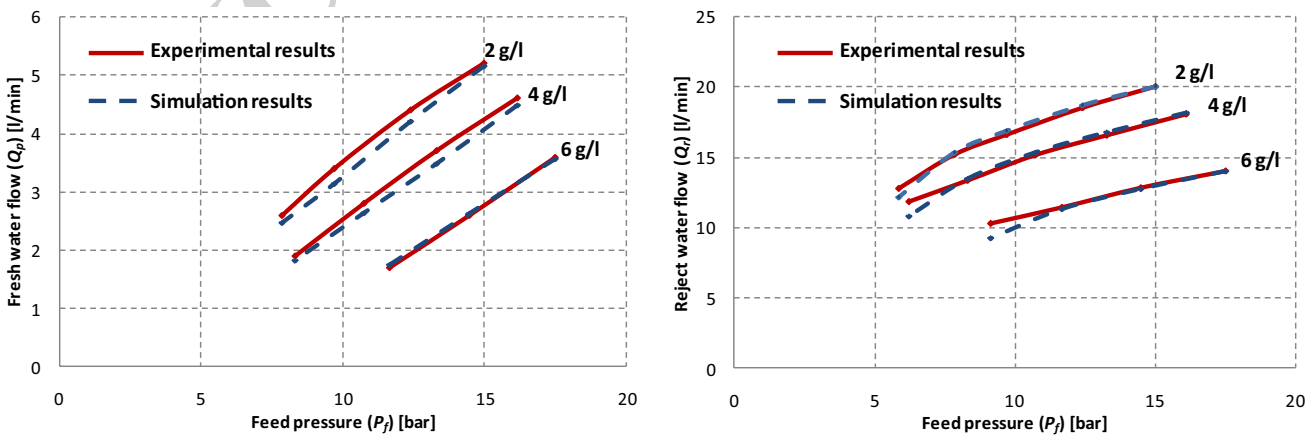

Fig. 6 Water flow rates as a function of feed pressure for different salinity levels

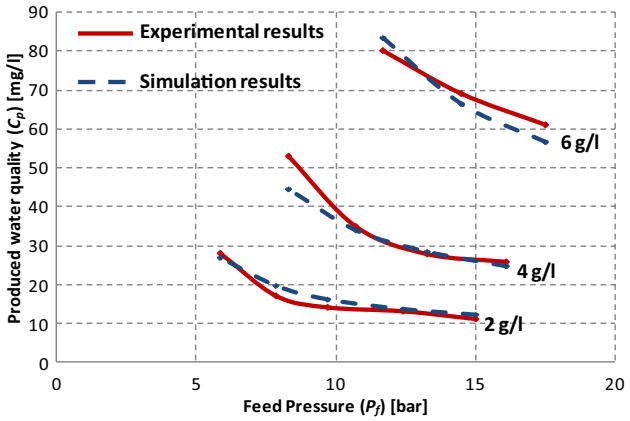

Fig. 7 Variation in produced water quality with feed water pressure

pressure and the desalination efficiency, demonstrating whether higher or lower pressures lead to variations in the salt concentration of the treated water. Further insights into these dynamics could contribute to optimizing the osmose inverse desalination unit for enhanced freshwater production efficiency.

The developed models exhibit excellent agreement with the practical testing carried out on the pilot desalination system, thus confirming, and affirming their reliability. This validation further enhances the confidence in the accuracy and effectiveness of the developed models, establishing them as robust tools for analysing and predicting the performance of the desalination system.

In the context of ensuring the system's stability and optimal performance, determining the SOW becomes crucial. This involves understanding the electrical power range and its impact on various components, enabling effective control, management, and energy sharing across the system to maximize output based on available electrical power.

By defining the SOW, the system can be operated within safe limits, considering the intermittent and variable nature of the electrical source, while maintaining the integrity of the water production and treatment process.

Safe Operating Windows (SOW) Steps

This section aims to establish the SOW limits for the water production and treatment process, considering a variable and intermittent electrical source. The objective is to ensure that the system operates within safe limits without compromising its components. The range of electrical power is crucial in determining the control and management approach, as well as optimizing energy utilization across system components.

Technological Constraints Establishment and numerical Modelling

The technological constraints are essentially related to the centrifugal motor-pump and the RO membrane which are the main parts in the system.

The centrifugal motor-pump constraints are listed in Table 4:

The membrane manufacturer's software is the only one that can be used for the design and operation of RO systems (Table 5).

Based on the previously indicated technological restrictions, a numeric model of the desalination process was created (Fig. 8). This numerical model may be used to simulate the operation of the motor-pump-HP and the BWRO membrane while utilizing a PFOC control technique [27]. Through this numeric model, comprehensive simulation tests can be conducted by manipulating all parameters of the motor-pump system in relation to the RO membrane. This capability allows for a thorough investigation of the system's performance under various conditions and facilitates the optimization of operational parameters for enhanced efficiency and productivity.

Simulation Results

The simulation results display regions indicated in green as permissible and those in red as inadmissible. Figure 9a depicts a SOW limit of 6 g/l feed water salinity at a 25°C temperature and a fixed CV position ($Y = 20\%$). The highest freshwater production is achieved with an electrical power of 1100W. However, exceeding this electrical power value

Table 4 Motor-pump constraints

Parameter	Typical value		Reason
Electrical power $\mathscr{P}$	max	2700W	Maximum power supported by the motor-pump
	min	130W	Minimum power required to pump water
ON/OFF period	max	–	–
	min	5 min	Prevent motor-pump destruction
Efficiency (η)	max	100%	–
	min	20%	Minimum efficiency accepted

Journal : Large 40866 | Article No : 189 | Pages : 18 | MS Code : 189 | Dispatch : 28-12-2023

Table 5 RO Membrane constraints

Parameter	Typical value		Reason
Feed pressure (P_f)	max	21 bar	Maximum pressure supported by the membrane
	min	1.26 bar	Osmotic pressure depends on the water salinity (1.26 bar for 25°C, 1500 mg/l)
Pressure drop (P_d)	max	1.4 bar	Prevent membrane destruction per vessel
	min	–	–
Feed flow (Q_f)	max	39 l/min	Maximum feed flow limit per vessel
	min	7.9 l/min	Ensure turbulent state to reduce polarization
Freshwater flow (Q_p)	max	4.5 l/min	Maximum freshwater flow limit per vessel Limit the flow to minimize fouling
	min	–	–
Reject water flow (Q_r)	max	38.2 l/min	–
	min	7.9 l/min	Minimum reject water flow limit per vessel Ensure turbulent state to reduce polarization
Recovery (Y)	max	20%	Reduce the risk of precipitation of salts, reduce polarization, maintain sufficient pressure in the membrane per vessel
	min	5%	Maximum cost limit
Freshwater salinity (C_p)	max	0.5 to 1g/l	Ensure an acceptable salinity
	min	–	–

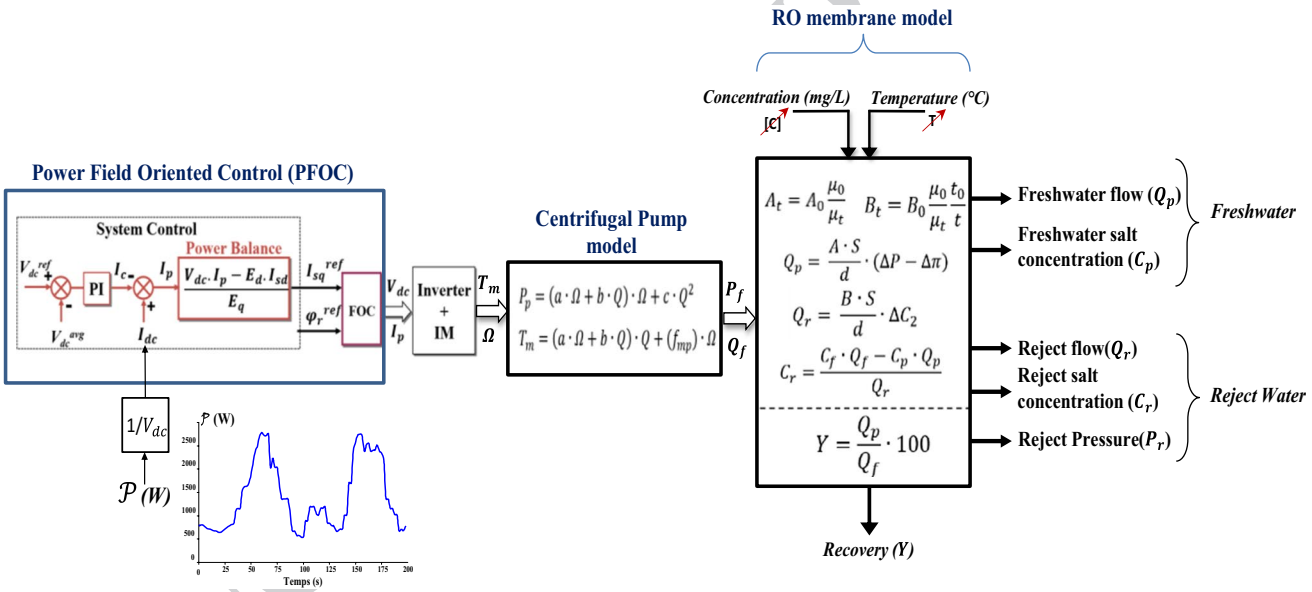

Fig. 8 Block diagram of the BWRO desalination model with PFOC control

can damage the membrane and surpass the manufacturer's maximum flow limit. Very low electrical power results in low recovery rates, making the desalinated water production less profitable.

By adjusting the CV while keeping the salinity and temperature constant, the recovery rate changes, and the load characteristic shifts to the right (lower $Y(\%)$ for the same electrical power) or left (higher $Y(\%)$ for the same electrical power). Figure 9b illustrates the SOW for multiple valve positions.

The SOW is limited by five curves:

(a) Qr_{min} =7.9 l/min (limited by the manufacturer regardless of the temperature);
(b) $Y_{min} = 5\%$ (set by the user);
(c) $Y_{max} = 20\%$ (limited by the manufacturer regardless of the temperature);
(d) $Qp_{max} = 4.3$ l/min (limited by the manufacturer regardless of the temperature);

Journal : Large 40866 | Article No : 189 | Pages : 18 | MS Code : 189 | Dispatch : 28-12-2023

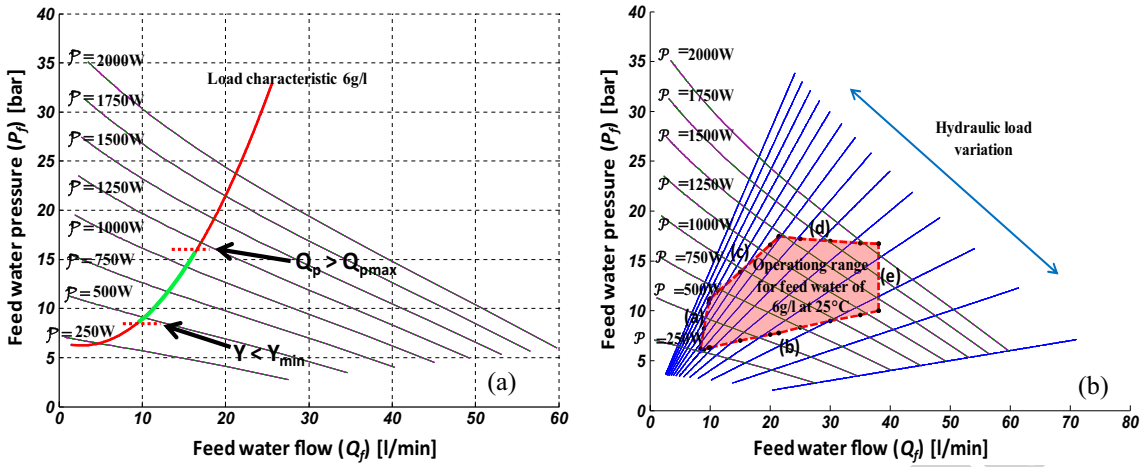

Fig. 9 SOW Limits determination

(e) $Qf_{max} = 38.1$ l/min (limited by the manufacturer regardless of the temperature).
(f) The SOW is a pentagon; each side represents a constraint not to exceed.

In the figures above, the load and iso-power characteristic curves are plotted. The operating point is the intersection of the load characteristic curve and iso-power curve.

The safe operating window (SOW) is depicted as a pentagon, with each side representing a constraint. The SOW defines the range of electrical power required for the system's operation. For instance, in the scenario illustrated in the figure, the maximum allowable motor-pump electrical power is 1070 W. Any value above this exceeds the scope and violates a constraint ($Q_p > Q_{p\max}$).

The next figures show the variation of the SOW according to the feed water salinity and feed water temperature (Fig. 10).

Elevating feedwater salinity corresponds to an augmented osmotic pressure. Consequently, a commensurate increase in feed pressure is imperative to initiate the RO phenomenon and facilitate freshwater production. The necessity for heightened pressure values elucidates the upward shift in the SOW, indicative of greater pressure requirements. Simultaneously, the SOW surface contracts with the elevation of feedwater temperature. This contraction implies a reduction in the fluctuation range of feed pressure from a hydraulic perspective and a decrease in the variation range of electrical power from an electrical standpoint. Such changes correlate with the observed rise in freshwater flow as temperature increases, leading to a concomitant decrease in the pressure

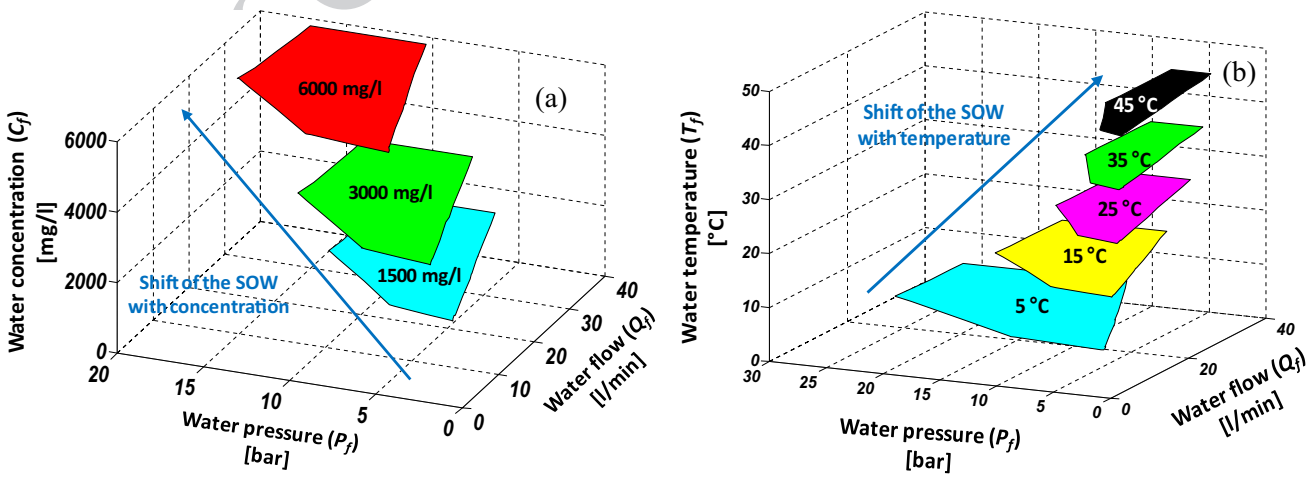

Fig. 10 Operating range variation according to feed water salinity (**a**) and Temperature (**b**)

Journal : Large 40866 | Article No : 189 | Pages : 18 | MS Code : 189 | Dispatch : 28-12-2023

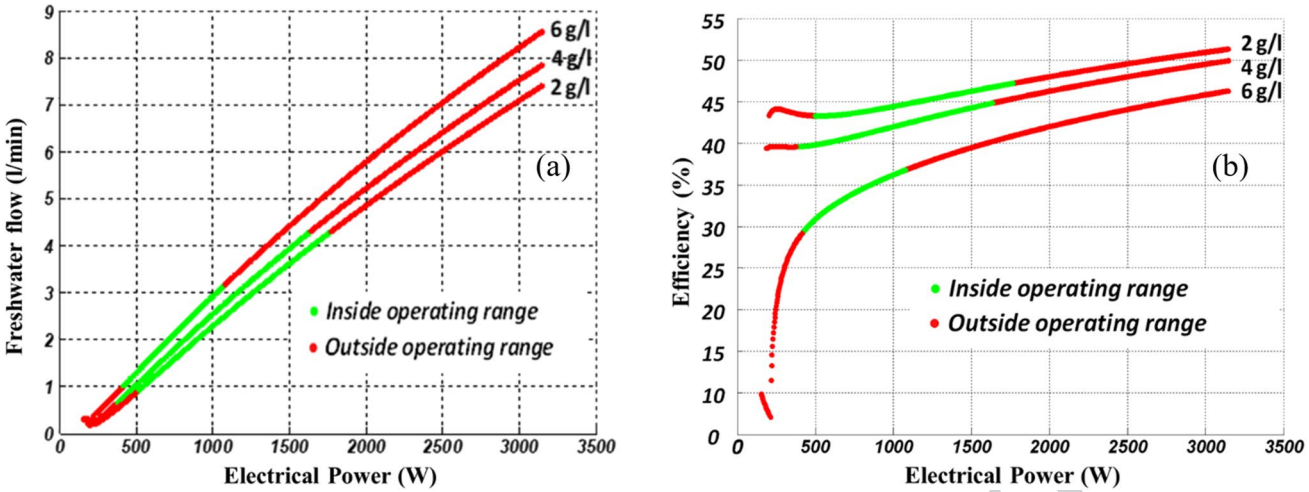

Fig. 11 Freshwater production (**a**) and Motor-pump efficiency (**b**) according to electrical power

required for achieving the maximum permissible freshwater flow (Qp_{max}).

Figure 11a depicts the evolution of freshwater production as a function of electrical power, as well as the electrical power range that allows work within the SOW (all constraints are respected). The electrical power range permitted for feed water with a salinity of 6g/l is [420W, 1070W]. If the goal was to maximize freshwater production, the process must operate at the highest power level possible within this range: which in this case is 1070W to create 3.15 l/min of freshwater.

Figure 13-b represents motor-pump-HP efficiency as a function of electrical power. To maximize motor-pump efficiency or water output, the system must operate with the highest value of power inside the SOW, which implies 1070W for 6g/l of feed water salinity with a motor-pump efficiency of 37%.

Power Sharing and Water-Energy management

Real-time Water-Energy management aims to maximise the amount of water produced while minimizing the energy consumption of the prototype desalination unit in accordance with the instantaneous electrical power supplied by the renewable hybrid microgrid under fluctuating climatic conditions. According to a predetermined profile, a fluctuating and intermittent electrical power supply drives this experimental process.

The first step in defining an acceptable Water-Energy management strategy is to analyse the BWRO desalination process's operating conditions and restrictions, especially given its energetic behaviour. The second step is to establish the degrees of freedom provided by the design to manage a comfortable system operation. Finally, an optimized Water-Energy management strategy contributes to the overall system's efficiency. This Water-Energy management is mostly dependent on the choice of electrical power sharing strategies between the two motor-pumps.

The proposed management strategy is primarily focused on a precise selection of the motor pump's control mode in accordance with the electrical energy supplied by the renewable source. Figure 12 shows a system management strategy in which energy as well as material (here, water amount) flows must be handled at the same time based on climatic conditions. For each inverter, two control solutions are proposed: Electrical power control and/or DC link voltage control.

It is possible to specify the control modes based on the electrical power available ($\mathcal{P}_{DC}$), the hydro mechanical properties of each motor pump inferred from the prototype's experimental findings, and the quantities of water (fresh and brackish) stored in the two reservoirs.

The fundamental step in power management relies primarily on an expert analysis system, leveraging the comprehensive understanding of the experimental prototype from its design phase and various conducted tests. This approach involves the allocation of electrical power to the motor-pumps based on the real-time power availability from the renewable source, employing predefined basic modes and limit intervals (Fig. 13). Therefore, each motor-pump will be within its acceptable operating range ($\mathcal{P}_{\text{pump-min}}$, $\mathcal{P}_{\text{pump-max}}$) while integrating the previously determined constraints and the SOW analysis.

Five separate modes provide a fundamental system supervision strategy:

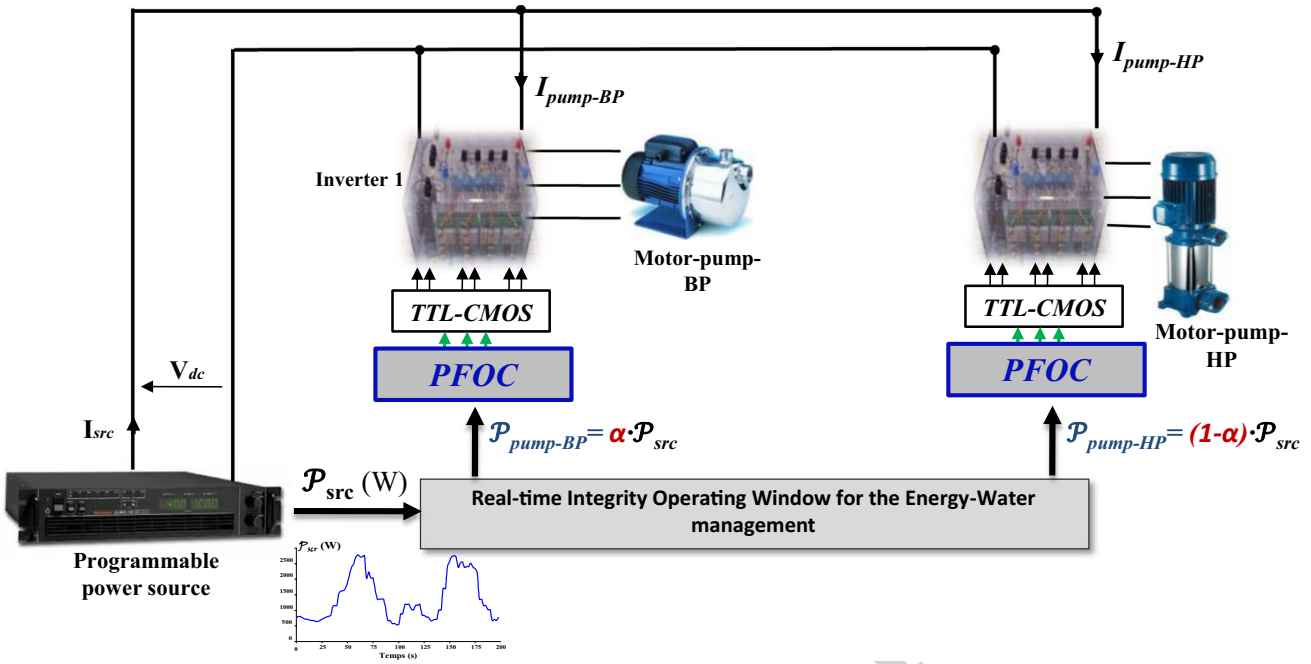

Fig. 12 Power management with PFOC control systems

Fig. 13 Basic EMS modes

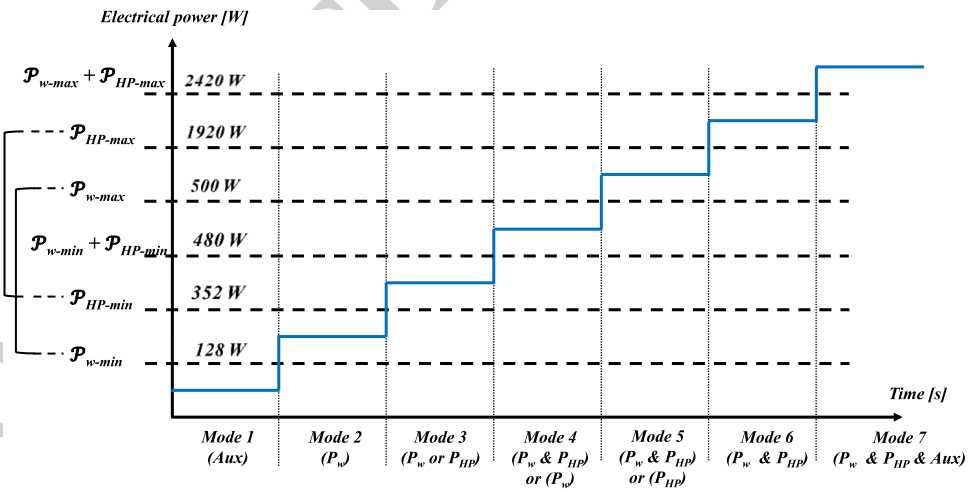

When the produced electrical power is sufficient to operate only one of the two motor-pumps, this approach allows for the utilization of modes 2 or 3 (corresponding to the WP and HP, respectively). In the absence of a battery, the DC link voltage is regulated by one of the voltage inverters, depending on the selected mode. This configuration introduces a higher degree of flexibility, enabling optimization of power sharing between the motor-pumps based on the efficiency of each power line.

In the fifth mode (PV, wind), the rated electric power of the two pumps exceeds the generated power. In such cases, the disparity in electrical power is balanced either by an auxiliary load or by downgrading the MPPT mode to ensure that each motor-driven pump operates at the same nominal power.

To evaluate the anticipated Energy-Water control and management performance following changes in operating modes, numerous tests were conducted on the BWRO desalination unit prototype, lasting over a duration of more than 200 s. The supervisor determines the management plan based on the operating modes. Figure 15a illustrates the power generated by the equivalent generator, while Fig. 15b depicts the DC bus voltage. The supervisor manager employs one of the three modes (modes 2, 3, and 4) to configure references and control modes for a specific real-time power profile.

Journal : Large 40866 | Article No : 189 | Pages : 18 | MS Code : 189 | Dispatch : 28-12-2023

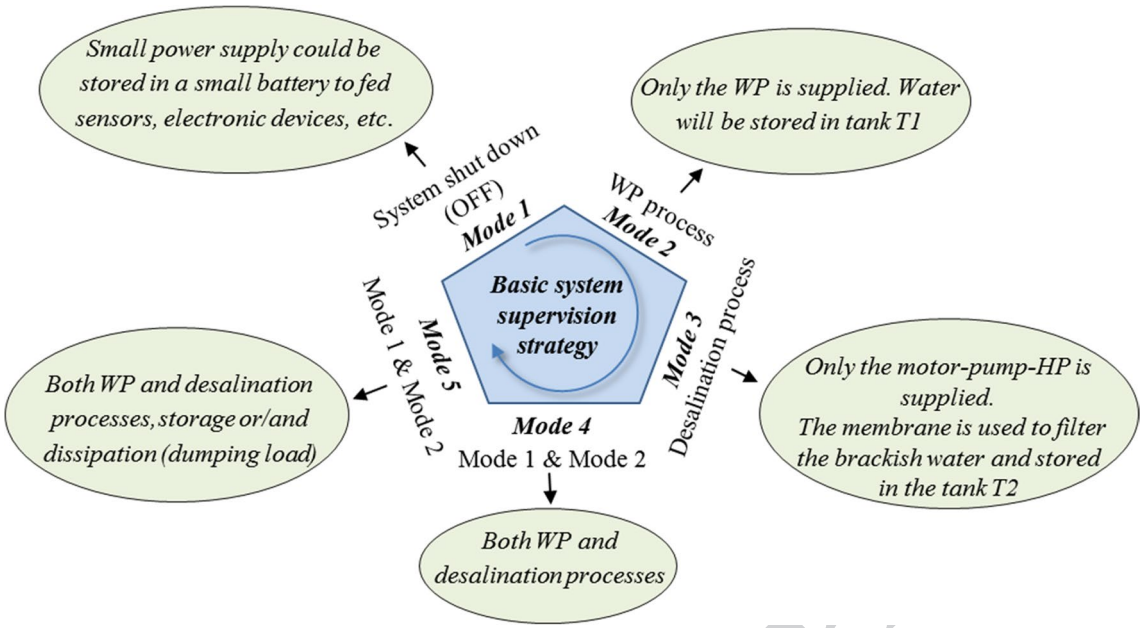

AQ12 **Fig. 14** Five basic modes for the Water-Energy management

AQ10 Figure 14c illustrates the feed water pressure (P_f), reject water pressure (P_r), and feed pressure operating limits. The feed water pressure (P_f), is always less than the operating limit of 21 bar. This is owing to the low salinity of the feed water (4.5 g/l). Osmotic pressure grows with salt, and feed water pressure must be adequate to offset osmotic pressure and enhance output freshwater flow. Figure 14d shows the fluctuation in pressure drop (P_d) as a function of motor-pump-HP electrical power. When the desalination motor-pump-HP to 1920 W, the pressure (P_d) reaches its maximum limit of 1.4 bar, which explains why this number was chosen for this experimental test. It may be determined that the greatest electrical power that can be supplied to the desalination process under these salinity, temperature, and recovery rate circumstances is restricted AQ11 by the pressure drop *(Pd)* maximum value limitation (Fig. 15).

Figure 16a depicts the variation of water flow rates across the RO membrane. The feed water flow rate (Q_f) corresponds to the highest flow rate, while the produced freshwater flow rate (Q_p) corresponds to the lowest flow rate. The reject and freshwater flow rates are characterized by a turbulent flow due to the high hydraulic load caused by the linked pipes, which may cause disturbances in the measurements obtained from the flow meters.

The operating constraints depicted in the same figure show that the feed and reject water flow rates are far from the extreme limits for this test. However, the freshwater flow rate (Q_p) reaches its maximum limit of 4.5 l/min when the motor-pump-HP operates at 1920 W.

Based on these experimental tests, we can conclude that for this test case, the two constraints defining the maximum electrical power ($\mathscr{P}_{\text{HP-max}}$), allowed for the operation of the motor-pump HP are the pressure drop (P_d) and the freshwater flow rate (Q_p). A second experimental test was conducted to determine the lower limit of electrical power that can be applied to the desalination processes. Under these salinity, temperature, and recovery rate (Y) conditions, the lower limit of electrical power is 352 W, at which the reject water flow rate (Q_r) reaches the lower limit of 7.91 l/min.

Figure 16b illustrates the variation of the recovery rate (Y) with respect to the provided electrical power. The recovery rate defines the efficiency of freshwater production in the RO desalination process. The adjustment of the control valve (CV) position enables the modulation of this rate. In this experimental trial, the position of the regulating valve is held constant, resulting in a consistent recovery rate during conventional operations. However, due to the variable nature of electrical power from renewable sources, the water flow rates will fluctuate, leading to a variable recovery rate even when the valve position remains fixed.

As can be shown, freshwater production is greatly influenced by the energy behaviour of the HP-pump. This study demonstrates that a RO desalination process can operate without the need for electrical storage, even in the presence of fluctuating electrical supply, as long as it stays within its technological limits. Unlike conventional systems, such as grid-connected setups or those with battery storage, this research provides compelling evidence that the desalination process can effectively harness variable electrical supply by optimizing and leveraging its inherent technological capabilities.

Journal : Large 40866 | Article No : 189 | Pages : 18 | MS Code : 189 | Dispatch : 28-12-2023

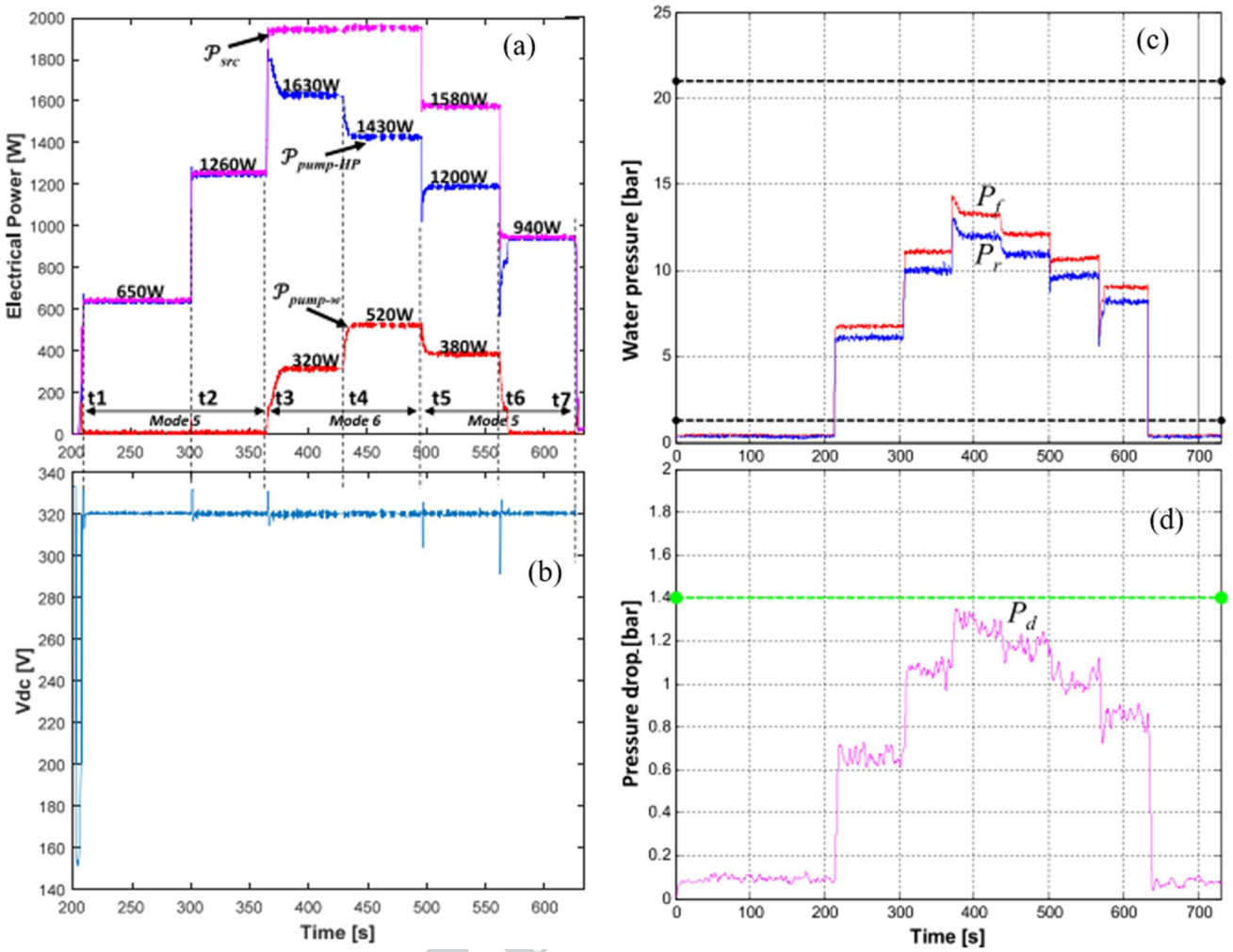

Fig. 15 Practical verification results for a variable power profile

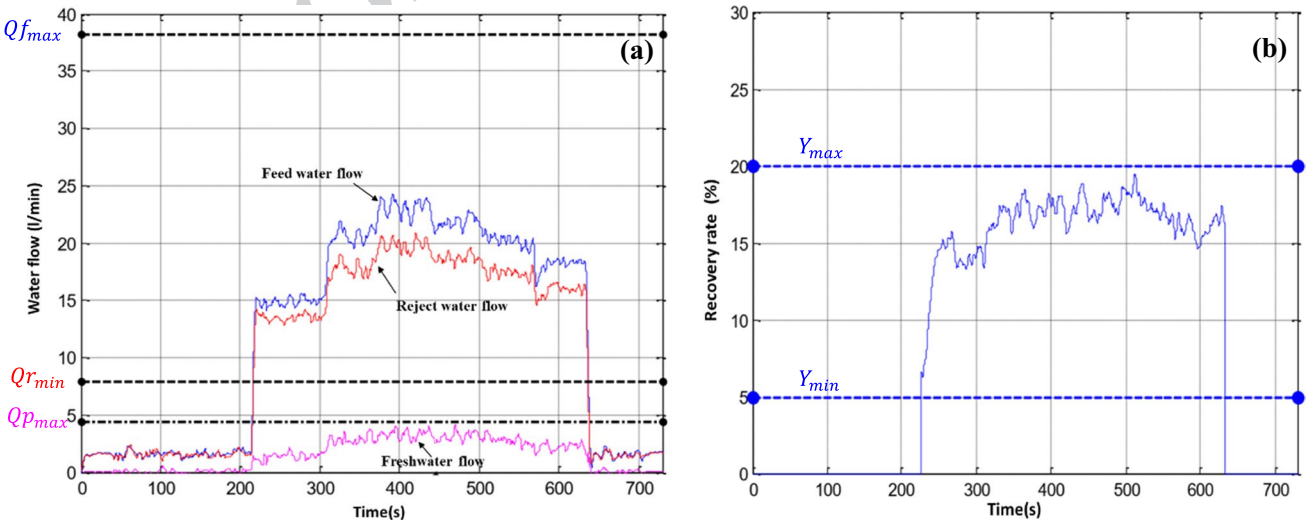

Fig. 16 Variation of water flow (**a**) and recovery (**b**) rates across the RO membrane

Journal : Large 40866 | Article No : 189 | Pages : 18 | MS Code : 189 | Dispatch : 28-12-2023

Conclusions

During this study, a static model of a Brackish Water Reverse Osmosis (BWRO) desalination unit was developed and experimentally validated, taking into consideration the technological constraints of the process. This model facilitates the investigation of the influence of electrical power variations on the performance of motor-pumps and the RO membrane in BWRO desalination. The establishment of a Safe Operating Window (SOW) and definition of an electrical power operating range ensure the reliable operation of the desalination unit, even when confronted with fluctuating electrical power, simplifying the control process.

Adhering to the specified operating range ensures the safe and efficient functioning of the system, even in the presence of fluctuations in hydraulic quantities at the RO membrane inlet. However, it is worth noting that the limits of the operating range should be adjusted considering factors such as brackish water salinity and temperature, as demonstrated in previous studies.

The implementation of autonomous RO water desalination systems powered by Renewable Energy Sources (RESs) in remote areas presents a significant challenge that warrants attention to ensure a sustainable freshwater supply. The water-energy nexus plays a pivotal role in this context, and the integrated approach proposed in this research, combined with a microgrid system, presents a viable solution to optimize the synergy between water and energy.

Furthermore, the developed model and energy management strategy contribute to the sustainable development of the ecosystem by maximizing freshwater production and minimizing energy consumption. This optimization process enhances economic viability by efficiently harnessing available resources and reducing reliance on external energy sources. This approach aligns with the principles of sustainable development, promoting a harmonious balance between economic, social, and environmental aspects.

Acknowledgements The authors would like to thank the Tunisian Ministry of Higher Education and Scientific Research, the UTIQUE-CMCU 12G1103 project and ERANETMED (H2020) European collaboration project "Energy and Water Systems Integration and Management" ID number 044, Energy-Water Nexus for supporting this work.

Data Availability The datasets generated and/or analysed during the current study are not publicly available due to the use of these data in a European project: ERANETMED (H2020) European collaboration project "Energy and Water Systems Integration and Management" ID number 044, Energy-Water Nexus. However, they are available from the corresponding author upon reasonable request.

Declarations

Conflict of Interest On behalf of all authors, the corresponding author states that there is no conflict of interest.

References

1. Billions of people will lack access to safe water, sanitation and hygiene in 2030 unless progress quadruples – warn WHO, UNICEF. https://www.who.int/news/item/01-07-2021-billions-of-people-will-lack-access-to-safe-water-sanitation-and-hygiene-in-2030-unless-progress-quadruples-warn-who-unicef. (Accessed 9 Jul 2023)
2. Qasim M, Badrelzaman M, Darwish NN et al (2019) Reverse osmosis desalination: A state-of-the-art review. Desalination 459:59–104. https://doi.org/10.1016/j.desal.2019.02.008
3. Curto D, Franzitta V, Guercio A (2021) A Review of the Water Desalination Technologies. Appl Sci 11:670. https://doi.org/10.3390/app11020670
4. Ahmed FE, Khalil A, Hilal N (2021) Emerging desalination technologies: Current status, challenges and future trends. Desalination 517:115183. https://doi.org/10.1016/j.desal.2021.115183
5. Lotfy HR, Staš J, Roubík H (2022) Correction to: Renewable energy powered membrane desalination — review of recent development. Environ Sci Pollut Res 29:46569–46569. https://doi.org/10.1007/s11356-022-20947-y
6. International Renewable Energy Agency. Water Desalination Using Renewable Energy, 2012 Technology Brief I12, Abu Dhabi, IRENA. Available online: http://www.irena.org/DocumentDownloads/Publications/Water_Desalination_Using_Renewable_Energy_-_Technology_Brief.pdf (Accessed June 17, 2023)
7. Healy RW (2015) The water-energy nexus–an earth science perspective. U.S. Geological Survey, Reston
8. Ahmadi E, McLellan B, Tezuka T (2020) The economic synergies of modelling the renewable energy-water nexus towards sustainability. Renew Energy 162:1347–1366. https://doi.org/10.1016/j.renene.2020.08.059
9. Okampo EJ, Nwulu N (2021) Optimisation of renewable energy powered reverse osmosis desalination systems: A state-of-the-art review. Renew Sustain Energy Rev 140:110712. https://doi.org/10.1016/j.rser.2021.110712
10. Ali E (2022) Optimal Control of a Reverse Osmosis Plant for Brackish Water Desalination Driven by Intermittent Wind Power. Membranes 12:375. https://doi.org/10.3390/membranes12040375
11. Miranda MS, Infield D (2003) A wind-powered seawater reverse-osmosis system without batteries. Desalination 153:9–16. https://doi.org/10.1016/S0011-9164(02)01088-3
12. Gilau AM, Small MJ (2008) Designing cost-effective seawater reverse osmosis system under optimal energy options. Renew Energy 33:617–630. https://doi.org/10.1016/j.renene.2007.03.019
13. Pohl R, Kaltschmitt M, Holländer R (2009) Investigation of different operational strategies for the variable operation of a simple reverse osmosis unit. Desalination 249:1280–1287. https://doi.org/10.1016/j.desal.2009.06.029
14. Park GL, Schäfer AI, Richards BS (2011) Renewable energy powered membrane technology: The effect of wind speed fluctuations on the performance of a wind-powered membrane system for brackish water desalination. J Membr Sci 370:34–44. https://doi.org/10.1016/j.memsci.2010.12.003
15. Park GL, Schäfer AI, Richards BS (2012) The effect of intermittent operation on a wind-powered membrane system for brackish water desalination. Water Sci Technol 65:867–874. https://doi.org/10.2166/wst.2012.912
16. Park GL, Schäfer AI, Richards BS (2013) Renewable energy-powered membrane technology: Supercapacitors for buffering resource fluctuations in a wind-powered membrane system for brackish water desalination. Renew Energy 50:126–135. https://doi.org/10.1016/j.renene.2012.05.026
17. Shen J, Jeihanipour A, Richards BS, Schäfer AI (2019) Renewable energy powered membrane technology: Experimental

investigation of system performance with variable module size and fluctuating energy. Sep Purif Technol 221:64–73. https://doi.org/10.1016/j.seppur.2019.03.004
18. Richards BS, Park GL, Pietzsch T, Schäfer AI (2014) Renewable energy powered membrane technology: Brackish water desalination system operated using real wind fluctuations and energy buffering. J Membr Sci 468:224–232. https://doi.org/10.1016/j.memsci.2014.05.054
19 Ruiz-García A, Nuez I, Carrascosa-Chisvert MD, Santana JJ (2020) Simulations of BWRO systems under different feedwater characteristics. Analysis of operation windows and optimal operating points. Desalination 491:114582. https://doi.org/10.1016/j.desal.2020.114582
20. Ruiz-García A, Nuez I (2020) On-Off Control Strategy in a BWRO System under Variable Power and Feedwater Concentration Conditions. Appl Sci 10:4748. https://doi.org/10.3390/app10144748
21. Ruiz-García A, Nuez I (2022) Simulation-based assessment of safe operating windows and optimization in full-scale seawater reverse osmosis systems. Desalination 533:115768. https://doi.org/10.1016/j.desal.2022.115768
22. Turki M, Ben Rhouma A, Belhadj J (2009) Experimental characterization of a Reverse Osmosis desalination process fed by hybrid power source. In: 2009 6th International Multi-Conference on Systems, Signals and Devices. pp 1–6. https://doi.org/10.1109/SSD.2009.4956790
23. Khiari W, Ben Rhouma A, Turki M, Belhadj J (2014) DSPACE implementation and experimentation of Power Field Oriented Control for motor-pump fed by intermittent renewable sources. In: 2014 International Conference on Electrical Sciences and Technologies in Maghreb (CISTEM). IEEE, Tunis, Tunisia, pp 1–6. https://doi.org/10.1109/CISTEM.2014.7077035
24. Khiari W, Turki M, Belhadj J (2016) Experimental prototype of reverse osmosis desalination system powered by intermittent renewable source without electrochemical storage: « Design and characterization for energy-water management». In: 2016 International Conference on Electrical Sciences and Technologies in Maghreb (CISTEM). IEEE, Marrakech & Bengrir, Morocco, pp 1–7. https://doi.org/10.1109/CISTEM.2016.8066819
25. Ben Ali I, Turki M, Belhadj J, Roboam X (2014) Systemic design of a reverse osmosis desalination process powered by hybrid energy system. In: 2014 International Conference on Electrical Sciences and Technologies in Maghreb (CISTEM). IEEE, Tunis, Tunisia, pp 1–6. https://doi.org/10.1109/CISTEM.2014.7076941
26. Ben Ali I, Turki M, Belhadj J, Roboam X (2016) Using quasi-static model for water/power management of a stand-alone wind/photovoltaic/BWRO desalination system without batteries. In: 2016 7th International Renewable Energy Congress (IREC). IEEE, Hammamet, pp 1–6. https://doi.org/10.1109/IREC.2016.7478871
27. Khiari W, Turki M, Belhadj J (2019) Power control strategy for PV/Wind reverse osmosis desalination without battery. Control Eng Pract 89:169–179. https://doi.org/10.1016/j.conengprac.2019.05.020
28. Ben Ali I, Turki M, Belhadj J, Roboam X (2020) Systemic design and energy management of a standalone battery-less PV/Wind driven brackish water reverse osmosis desalination system. Sustain Energy Technol Assess 42:100884. https://doi.org/10.1016/j.seta.2020.100884
29. Barello M, Manca D, Patel R, Mujtaba IM (2015) Operation and modeling of RO desalination process in batch mode. Comput Chem Eng 83:139–156. https://doi.org/10.1016/j.compchemeng.2015.05.022
30. Bilton AM, Wiesman R, Arif AFM et al (2011) On the feasibility of community-scale photovoltaic-powered reverse osmosis desalination systems for remote locations. Renew Energy 36:3246–3256. https://doi.org/10.1016/j.renene.2011.03.040
31. Kumarasamy S, Narasimhan S, Narasimhan S (2015) Optimal operation of battery-less solar powered reverse osmosis plant for desalination. Desalination 375:89–99. https://doi.org/10.1016/j.desal.2015.07.029
32. Sassi KM, Mujtaba IM (2013) Optimal operation of RO system with daily variation of freshwater demand and seawater temperature. Comput Chem Eng 59:101–110. https://doi.org/10.1016/j.compchemeng.2013.03.020
33. Sobana S, Panda RC (2011) Review on modelling and control of desalination system using reverse osmosis. Rev Environ Sci Biotechnol 10:139–150. https://doi.org/10.1007/s11157-011-9233-z
34. Sundaramoorthy S, Srinivasan G, Murthy DVR (2011) An analytical model for spiral wound reverse osmosis membrane modules: Part I — Model development and parameter estimation. Desalination 280:403–411. https://doi.org/10.1016/j.desal.2011.03.047
35. Ahmad N, Sheikh AK, Gandhidasan P, Elshafie M (2015) Modeling, simulation and performance evaluation of a community scale PVRO water desalination system operated by fixed and tracking PV panels: A case study for Dhahran city, Saudi Arabia. Renew Energy 75:433–447. https://doi.org/10.1016/j.renene.2014.10.023